

Modeling Currents About Vitellogenic Oocytes of the Cockroach, *Blattella germanica*

J. G. KUNKEL AND E. BOWDAN

Zoology Department, University of Massachusetts, Amherst, Massachusetts 01003

Abstract. An insect oocyte with a disc-shaped sink of current on its ventral surface during a vitellogenic phase of development is used to demonstrate modeling of expected currents arising from a mathematically defined source. A simple model with an analytical solution for the expected currents is compared to a more complex model in which expectations are computed by mathematical integration. The currents about two oocytes of different pattern type are interpreted in light of the two models.

Introduction

Ionic currents surrounding an insect oocyte may have a role in the physiology and development of the future embryo (Jaffe, 1986). The vibrating probe makes it possible to describe such currents in terms of their spatial pattern and intensity. During vitellogenesis the cockroach oocyte, a simple panoistic insect oocyte, has a sink of inward current at its ventral surface and a complimentary exit of current more broadly from the dorsal surface (*cf.*, Kunkel, 1986; Kunkel *et al.*, 1986). However, because the probe is non-invasive and is vibrating, current is measured at positions remote from the actual cell membrane. Typically the probe vibrates one probe diameter, making it in fact impossible to approach a source closer than $25\ \mu$ with the center of vibration of a $25\text{-}\mu$ probe. Thus, a display of fields of current vectors measured at any distance from the oocyte gives an incomplete characterization of even this relatively simple pattern with respect to the cell surface. This is because current measurements made at discrete positions remote from the cell surface are weighted integrations of current from all membrane sources, with local sources more heavily weighted for two reasons: first, as indicated by equation (1) the contribution of current from each point on the cell falls off with the square of its distance from

the measuring point and second, only the components in the directions of the probe's two vibration axes are measured.

It is crucial to understand the relationship between measured current patterns in the medium and current sources flowing through a membrane. With such an understanding, rapid and repeated sampling of current fields about cells would then lead to knowledge about the patterned ionic flux through the membrane and hence through the cell.

So far the mathematics of patterns of currents has only been applied by a few investigators in the field, and only in simple cases (Jaffe *et al.*, 1974; Betz and Caldwell, 1984). Freeman and *et al.* (1985) examined a more complex model. We introduce here an attempt to establish an approach with a slightly more complex system that changes over time. We expect this will lead to the sequential building of mathematical models, which will allow us to describe the current properties of any membrane system examined by means of the non-invasive vibrating probe technique.

Making sense of these fields of currents requires practice with simple models of hypothesized phenomena. Often, examining physical and mathematical models of the patterns and strengths of currents about well-defined, three-dimensional objects allows more insights than can be achieved by examining non-ideal natural examples. However, the models will only provide insight when they accurately describe and predict natural phenomena.

If current, i , emanates from a single point source, as is the case for one standard calibration procedure, then the radial current density 'I' is inversely proportional to the square of the radial distance 'k' from the source:

$$I = i/(4 \cdot \pi \cdot k^2) \quad (1)$$

In an isotropic medium then, potential drops perceived by the probe can be automatically interpreted as

current densities at the probe's position. This simple model does not estimate current density at the 'point' source, much less from multiple point or irregularly shaped sources. However this formula (1) can be used in conjunction with a model or knowledge of current patterns passing through a particular source, to integrate, on a point-by-point basis, what the current density measurable at some external point should be. For the orifice of a glass electrode used to inject a known current the inverse calculation of the source current density is simple, dividing the total current on the sphere of radius 'k' by the area of the orifice. Integration formulae have been developed predicting local currents remote from simple non-point sources (Freeman *et al.*, 1985; Purcell, 1985). The inverse operation of predicting what the source is like based on remote measurements is the crux of biological use of the vibrating probe. We examine two models of disc sources of current and apply these models to interpreting the disc-shaped sinks of current we hypothesize to be on the ventral surface of cockroach oocytes.

Materials and Methods

Measurements of current density around, and at different distances from, oocytes were made using the 2-D vibrating probe at the National Vibrating Probe Facility, Woods Hole. The medium used was a simplified version of Landureau's tissue culture medium and contains 4 mM CaCl₂; 14 mM KCl; 5 mM MgSO₄; 145 mM NaCl; 11 mM H₃PO₃, to buffer the medium at pH 6.8; 110 mM sucrose, to give an osmolarity of 390 mOsm; 12.5 mg/100 ml penicillin; 0.5 mg/100 ml streptomycin. Individual ovarioles of the German cockroach, *Blattella germanica*, were dissected, in this medium, from first parturition females which had access to food for 2–5 days. [Growth of oocytes is initiated by feeding the females at 30°C, the temperature for the maximum growth rate of this species. Newly metamorphosed females, which have been fed for 4 days, for example, have oocytes approximately 2/3 of the way through the vitellogenic phase, measuring 1.2–1.3 mm, and will be ovulated in 2 days (Kunkel, 1973)]. A single ovariole was dissected from an ovary and was then carefully positioned in an 8-ml plastic petri dish filled with medium. A layer of mineral oil over the medium's surface prevented evaporative convection of the medium. A heating coil and thermal probe in the oil layer maintained the preparation at 30°C. Oocytes prepared in this manner have exhibited stable currents for up to 10 h.

An XYZ coordinate system describes location. The X dimension is parallel to the length of the oocyte. Positive x-values are anterior, negative are posterior relative to the adult and the future embryo. The Y dimension defines the dorsal ventral axis of the future embryo, ventral

values being positive and dorsal negative. The X-Y plane with $z = 0$ is defined as the mid-sagittal plane through the oocyte. The Z dimension is lateral.

Two oocytes provided the data used in this study (Fig. 1). Although similar in size this time represents a transition in the current pattern which is correlated with oocyte growth. One (oocyte #1, 1.1 mm) was probed repeatedly close along the ventral mid-sagittal surface. Current densities from the other (oocyte #2, 1.2 mm) were first measured also close along the ventral mid-sagittal surface. Subsequent measurements were then made at various distances away from the surface, in the mid-sagittal plane. Additional measurements were made close to the oocyte to check that the currents remained stable. The data collected consisted of the x, y, and ($z = 0$) position of the probe, and the resolved x- and y-currents, I_x and I_y . From I_x and I_y the mid-sagittal total current, I_t , and the angle of the resultant current vector in the X-Y plane were calculated; these are plotted in Figure 1. This 'total current' cannot include an I_z component since the probe does not vibrate in that direction. Thus the I_t vector for the 2-D vibrating probe describes only two of the three dimensions of measurable current at a point in space remote from a three-dimensional source. However, I_x and I_y do benefit from point sources located in the Z direction (Fig. 3.)

Data from the PDP 11/23 system at the NVPF was captured on an MS/DOS computer configured as a terminal of the PDP 11/23 and stored on floppy disc. Further data analysis was made with a 80286 computer fitted with a 80287 math coprocessor using both commercial and custom designed software. MathCad was useful for numerical integrations of equations using circular coordinates. Custom software included a vector and cell outline plotting program and a contour fitting program written in Turbo Pascal.

Results

The first model that was examined is described by the equation:

$$I_y = 2 \pi I_r (1 - [k/\sqrt{k^2 + a^2}]) \quad (2)$$

which predicts the current, I_y , measured remote from a disc shaped source of radius 'a', current density ' I_r ' at radial distance 'r' on the disc surface, at a distance 'k' along the Y-axis normal to the center of the disc at (x, y, z) = (0, 0, 0) (Purcell, 1985). Along this axis both I_x and I_z are zero. Thus, the true total current is equivalent to both I_t and I_y . It should be noted that in this model, and also in model II, that I_r is a constant for $r < a$; but this could change in future models in which a non-uniform disc is considered. Relative to the central axis, the disc source is radially symmetric and thus the integral equations are

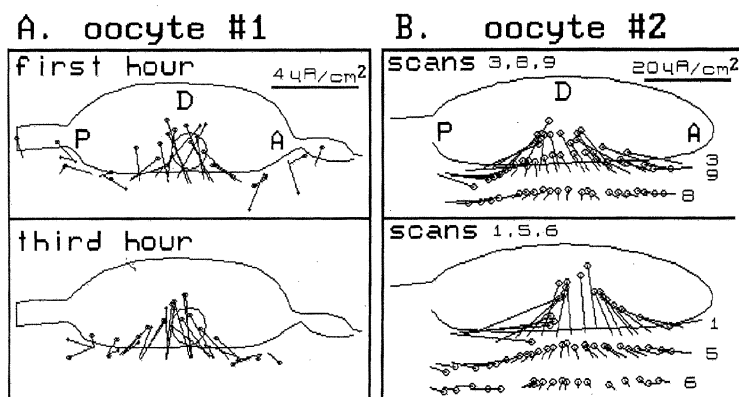


Figure 1. Outlines of two oocytes with local total current density vectors measured with a 2-dimensional vibrating probe. A circle marks the head of each vector. The base of each vector indicates the point of measurement. The length and direction of the displayed vector are computed as the sum of the x- and y-current vectors. A scale bar in the upper right corner for each oocyte indicates the vector calibration. (A) Oocyte #1 (1.1 mm)—repeated scans close to the mid sagittal ventral surface. (B) Oocyte #2 (1.2 mm)—measurements made at various distances away from the mid sagittal ventral oocyte surface. N. B. The current vectors of these oocytes are an order of magnitude smaller than those of Kunkel (1986). The discrepancy is due to an error in a computer program being developed at the earlier time. This error has since been corrected.

simple and can be solved analytically. Equation (2) is that analytic solution (Purcell, 1985).

In applying model I to experimental situations the distance, k , from the surface and the current I_y at position $(x, y, z) = (0, k, 0)$ are measurable. The radius and density of the current source on the surface are estimated by fitting the 'a' and 'I_r' parameters of equation (2) to observed (k, I_y) data. The greatest current density, I_y , emanating from oocyte #2 was measured in the central region. Total current densities at positions above the surface measured from this region were fitted to equation (2) and the radius of the disc source was calculated to be 125μ and current density on the disc to be $3 \mu A/cm^2$. The data fit well to the theoretical curve (Fig. 2) with the exception of those values measured during the first and last (9th) scans. Fit of scans 1 and 9 are substantially improved if a linear time-dependent decay rate (1/3 per h) is added to the equation. Measurement ended after scan 9 because it became obvious that the currents had begun to deteriorate at that time. Deterioration is evident from the positions of these data with respect to the theoretical curve, scan 1 data lie above the curve, scan 9 lie below. Model I cannot be fit to oocyte #1 data since scans were not done at varying distances from the source.

Subsequently, model II, a more flexible and complex extension of model I, was examined. This first step in increasing complexity is described by equations (3) and (4), which are based on Figure 3. They describe the normal, I_y , and tangential, I_x , currents measured along the X-axis at a distance y above a model disc of uniform current density. With $x = 0$, model II is identical to model I; but when x is not equal to zero, the equations to be

integrated are not rotationally symmetric, have no analytic solution, and thus must be integrated mathematically. Equations (3) and (4) allow the estimation of I_y and I_x at any point off the central axis by means of point-by-point mathematical integration of the current coming from all points $(x, 0, z)$ on a source surface measured at the point (x, y, z) (Fig. 3). In practice, since the model disc's source is symmetric about $(x, y, z) = (0, 0, 0)$, computations were simplified by making computations only for external points in the X-Y plane in what would correspond to the mid-sagittal plane of an oocyte, $z = 0$. Theoretical isopotential lines generated by these equations are shown in Figures 4 and 5. These figures demonstrate very clearly that I_x has maxima and minima corresponding to the edges of the disc source. Figure 5A especially shows that these peaks can be diagnostic of the size of this disc. In addition, the model of total current, $I_t = I_x + I_y$, predicts a plateau for large diameter discs probed close to the surface (Fig. 5B). In this case close would correspond to a distance that is a small fraction of the probed disc diameter, 2 units for a radius 10 disc.

Model II expectations were applied to the observed data from oocytes 1 and 2 (Fig. 6). The data from oocyte #1 are shown in Figure 6A. The plot of tangential current, I_x , shows clear maxima and minima indicating, if model II is accurate, that the source of inward current has a diameter of about 500μ . This value correlates well with the size implications of Figure 1. However, for this oocyte, minimum I_x is not symmetric with maximum I_x , as an ideal disc would exhibit. This suggests that the effective source (that is, either its shape or the distribution of pumps or channels) is not a perfect disc nor mir-

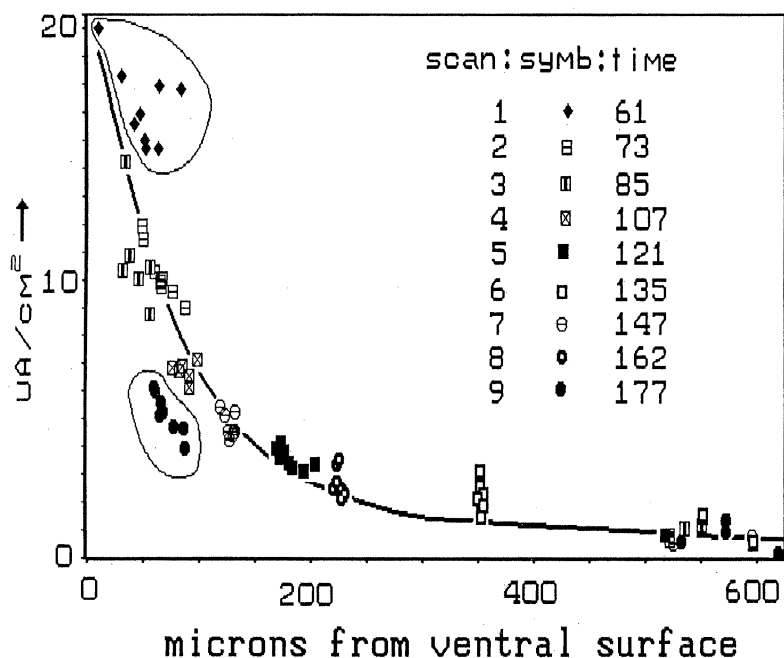


Figure 2. Theoretical current density generated by equation (2) (see text), using a disc source radius 125μ and a source current density of $3 \mu\text{A}/\text{cm}^2$, is plotted as a solid line. The observed data of oocyte #2 are superimposed. Each scan is plotted using a distinct symbol and the start time of the scan is tabulated in minutes from dissection time. The outlined measurements above and below the curve are those of scans #1 and #9 respectively (see text).

ror symmetric along the X-axis. This is supported by the plot of I_y , the normal current, which shows a displaced maximum. The relatively sharp peak of I_y also suggests that the maximum inward current is highly focused in this oocyte. No plateau of the total current, I_t , is perceived, additional support for the suggestion that the disc is non-uniform. The size of the disc is large enough such that probing at the typical distance from the ovariole surface, 35μ , at the disc center should result in a measured current density in the medium about 5–6 times the membrane level current density. This would suggest that the true current density at the disc center of oocyte 1 is closer to $0.5\text{--}1 \mu\text{A}/\text{cm}^2$ and closer to $3 \mu\text{A}/\text{cm}^2$ for oocyte 2.

Plots of scan 1 data from the second oocyte (Fig. 6B) suggest a differently shaped source. The plots of I_x have no sharply defined maxima and minima, which suggests that there is inward current across the major part of the ventral surface (*i.e.*, $900\text{--}1000 \mu$) and it is not focused. This is in contradiction to the prediction of model I (which suggested a source 250μ in diameter) but correlates more reasonably with what is intuitively observed in Figure 1. Again, minimum I_x is not quite symmetric with the maximum I_x . The plot of I_y has a broad plateau, which again indicates that the center of inward current is not focused. Plots of I_t for this oocyte are flat, indicative of a broad and relatively uniform unfocused current

source. In comparing oocyte 1 and 2, the membrane level current grew from 1 to $3 \mu\text{A}/\text{cm}^2$ and the area of the inward current increased by a factor of 2–3. The trend suggested by these two exemplars was observed overall in a substantially larger sample of oocytes, which will be reported elsewhere in a developmental context.

Discussion

Adequate interpretations of non-invasive physical measurements about cells depend upon appropriate models of the sources. Model I, equation (2), describes the decay of current along the normal axis, perpendicular to the center of a disc source and yields an estimate of the radius and the current density of the disc. It is sensitive enough to indicate deterioration of the source, but it has some restrictive limitations. The first is that measurements must be made along an axis normal to the cell surface, a position and direction that may be difficult to know under experimental conditions or that may shift with time or with changing conditions. We know that the borders of the disc (current reversal from inward to outward) shifts somewhat from scan to scan; but we do not yet know whether this, for example, corresponds to shifts in the center of the disc or to local changes in the disc border. The second limit of model I is that only the average radius of a source can be sensed so that asym-

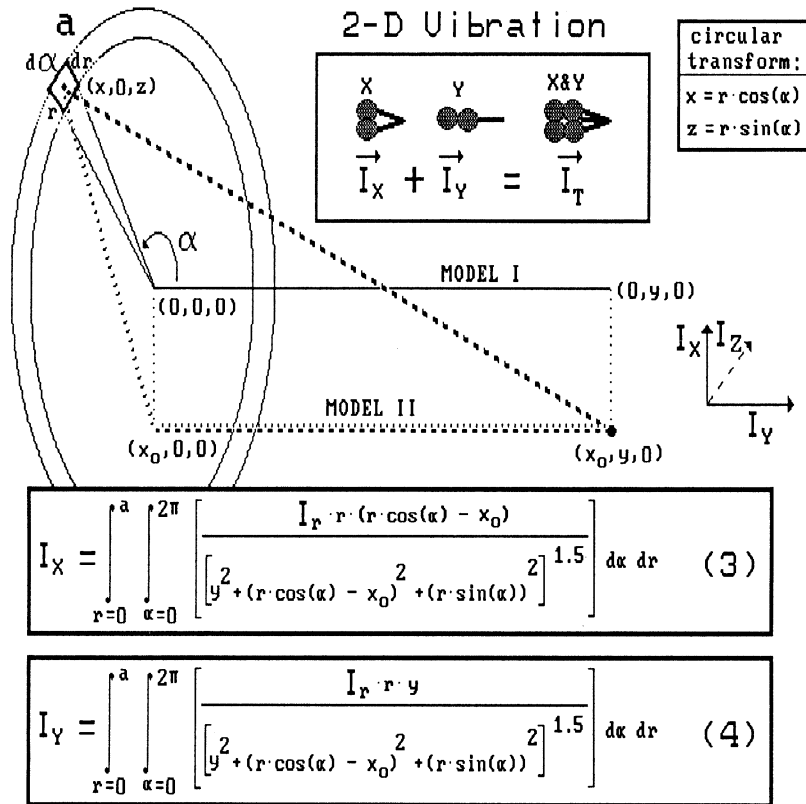


Figure 3. Physical model for equations (3) and (4). These indicate the 3-D disc source located on the ventral surface of a hypothetical oocyte measured by the probe in 2 dimensions: X, Y, Z—the three dimensions of space. A disc source of current is located in the X-Z plane on the ventral oocyte surface with its center at $(x, y, z) = (0, 0, 0)$. X is parallel to the length of the oocyte on which the disc is located. Y is normal to the disc at its center. The X and Z axes are tangential to the disc surface. The vibrating probe vibrates in two dimensions, X and Y only. The X coordinate at the point of measurement is designated x_0 . A dashed line outlines a right triangle in 3-space whose legs are y in the Y-dimension, $(r \cdot \cos(\alpha) - x_0)$ in the X-dimension and $(r \cdot \sin(\alpha))$ in the Z-dimension.

α = angle, in radians, used to transform the XZ coordinates $(x, 0, z)$ into circular coordinates (α, r) .

a = radius of the disc, in arbitrary units.

r = the radius at a particular point on the source.

$I_r = 1 \mu A / (\text{area unit})^2$ for $r < a$, the current density through the disk at a particular radius, r .

metries such as those suggested by departures from the more complex model II cannot be demonstrated. Equation (2) is limited to relatively small discs on a cell surface because distortions of a disc, due to, for example, cell curvature, will lead to substantial departures of the predicted curve from ideal behavior. Since the theoretical curve (2) has only two parameters dictating its form, it is difficult to ascribe departures in the shape of the curve to a particular departure of a disc from its ideal form.

Equations (3) and (4) describing model II are more robust in their ability to detect a divergence of observed data from ideal predictions and are, in general, more informative. The equation of the tangential current I_x (3)

indicates the limits of the source independently and so can detect an asymmetric source. For small disc sources the equation for current normal to the disc surface, I_y (4), provides a means of calculating the membrane-level current. Point-by-point integral equations can model irregularly shaped sources limited only by the ingenuity of the defining equations for the surface of integration and the current density function, $I_r = I(x, 0, z) = 1 \mu A / \text{cm}^2$ for $r < a$ in this case. Such an ability to model currents is necessary to relate patterns of remotely measured currents to the distributions and densities of functioning ion channels and pumps. Application of model II to the data collected from the two oocytes indicates that the sink of

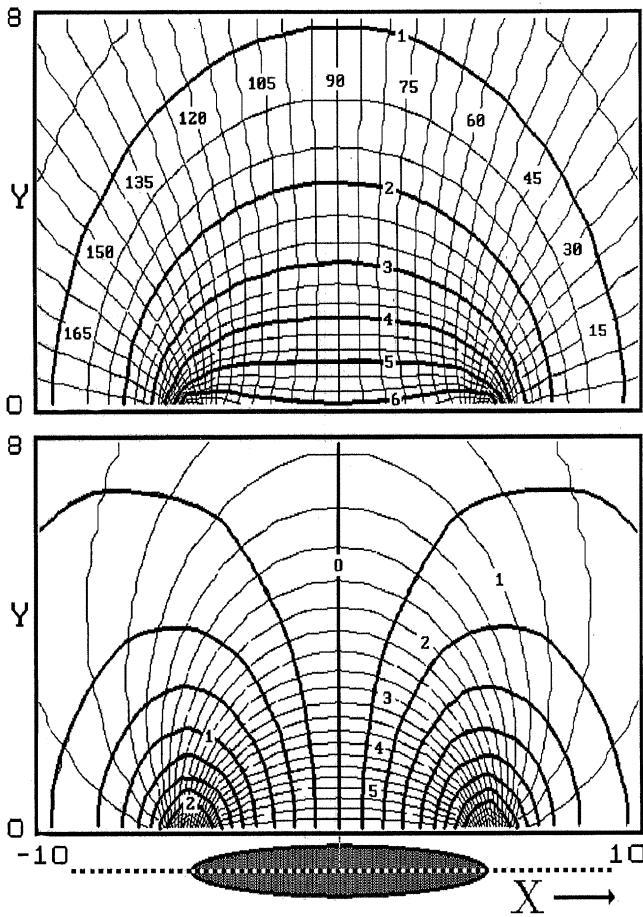


Figure 4. Predicted currents, generated from equations (3) and (4): current density at source held at $1 \mu\text{A}/\text{unit}^2$ on a disc of radius 5 units. (Bottom Panel) Isopotential contours for tangential, (I_x , thick contours) and normal, (I_y , thin contours) current densities. Below the contour plot is a representation of the disc source; a dotted line through the disc represents the location of the scan. (Top Panel) Isopotential contours for total current density (I_t , thick contours) and contours of equal angles (thin contours) subtended by the vectors.

inward current from the smaller oocyte is smaller and more tightly focused than that from the larger oocyte. This may be simply interoocyte variability or it may be a developmental change. Clearly, however, model II can quantitate the difference.

Thus, model II provides substantially more information than model I and allows for relatively easy extension to more complex models. However, it too has its limitations. Like the first model, it may overestimate current density at the disc surface by as much as $2 \cdot \pi$. This is because measurements made include substantial lateral contributions especially when the disc radius is large, even if the measurements are made as close to the surface of the disc as possible (1 probe diameter). This corruption of local measurements by lateral components argues

for routine measurement of the decay of current away from the surface to increase the ability to use modeling to predict the shape of the current source. A greater density of measurements at closer intervals along the surface can achieve similar ends. Sparse data are difficult to model with high resolution. In particular, geometric conditions increasing the number of measurements of either I_y or I_x may be preferable. As in model I, model II equations (3) and (4) assume a flat disc source while the oocyte surface is, of course, curved. Thus, we need to develop models that take more advanced geometry into account. This is not a difficult problem when mathematical integration is used as we did for model II. In spite of these limitations, model II is able to improve our interpretation of the observed currents about oocytes #1 and #2. It further provides an approach by which subtle changes of current pattern measured during develop-

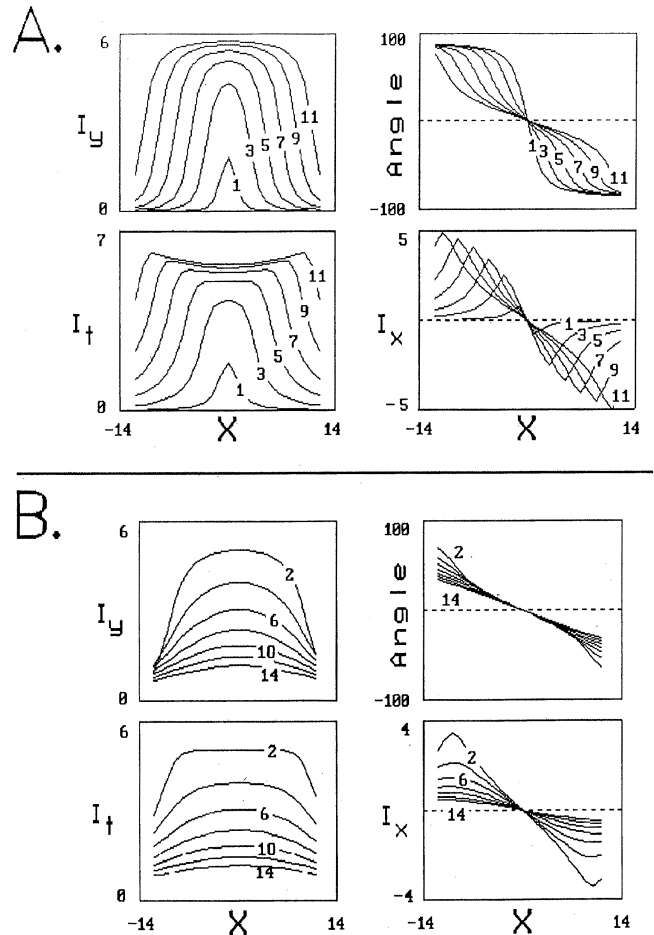


Figure 5. Calculated current densities: current density at source = $1 \mu\text{A}/\text{unit}^2$; measured along the X axis: (A) I_x , I_y , I_t and the angles of the vectors from discs of radius 1-11 arbitrary units; at 1 distance unit above the disc source. (B) I_x , I_y , I_t and angles from a disc, radius 10 units; predicted for 1 to 14 Y distance units above the disc source.

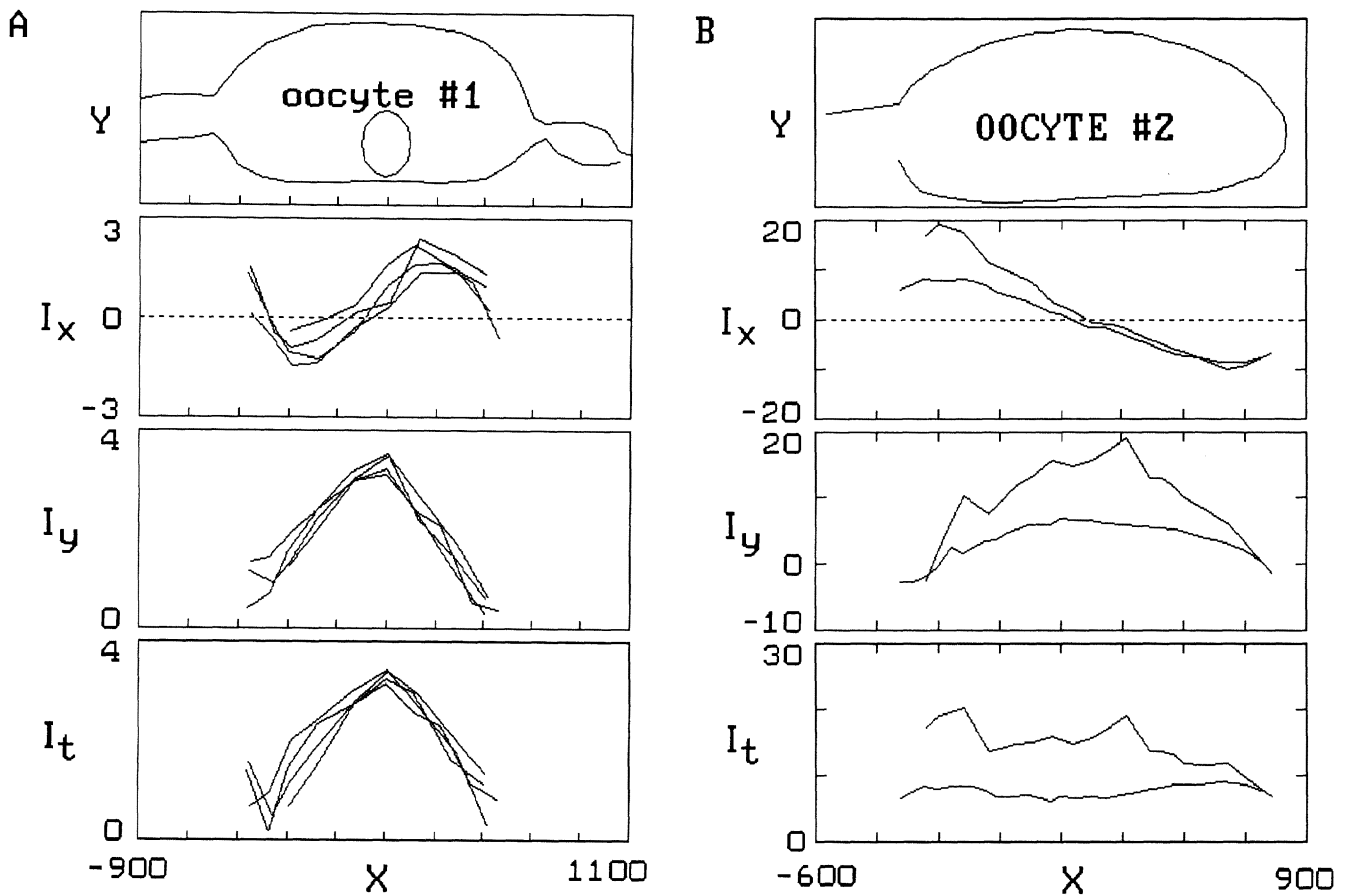


Figure 6. Observed data interpreted according to the model of I_x , I_y and I_t plotted under oocyte outlines for (A) Oocyte #1; (B) Oocyte #2

ment or caused by experimental manipulations may be interpreted with greater insight. Thus, a better understanding of the physiology of the oocyte should be possible.

Acknowledgments

We are grateful to Dr. L. Jaffe and the staff of the NVPF, especially A. Shipley and S. Dixon. This work was supported in part by NSF grant #DCB-851781

Literature Cited

- Betz, W. J., and J. H. Caldwell. 1984. Mapping electrical currents around skeletal muscle with a vibrating probe. *J. Gen. Physiol.* **83**: 143-156.
- Freeman, J. A., P. B. Manis, G. J. Snipes, B. N. Mayes, P. C. Samson, J. P. Wikswo, and D. B. Freeman. 1985. Steady growth cone currents revealed by a novel circularly vibrating probe. *J. Neurosci. Res.* **13**: 257-283.
- Jaffe, L. F. 1985. Extracellular current measurements with a vibrating probe. *TINS-December 1985* **8**: 517-521.
- Jaffe, L. F. 1986. Ventral activation process in insect oocytes. *Nature* **321**: 386.
- Jaffe, L. F., K. Robinson, and B. F. Picologlou. 1974. A uniform current model of the endogenous current in an egg. *J. Theor. Biol.* **45**: 593-595.
- Kunkel, J. G. 1973. Gonadotrophic effect of juvenile hormone in *Blattella germanica*: a rapid, simple quantitative bioassay. *J. Insect Physiol.* **19**: 1285-1297.
- Kunkel, J. G. 1986. Dorsoventral currents are associated with vitellogenesis in cockroach ovarioles. Pp. 165-172 in *Ion Currents in Development*, R. Nuccitelli, ed. Alan R. Liss, NY.
- Kunkel, J. G., R. Koenig, H. Kindle, and B. Lanzrein. 1986. Ion Flux during vitellogenesis and patterning of insect oocytes. *Adv. Invert. Reprod.* **4**: 101-108.
- Purcell, E. M. 1985. Electricity and Magnetism. *Berkeley Physics Course*, Vol. 2, 2nd edition. 484 pp. McGraw-Hill, NY.